# Supporting Information

## Nasuno et al. 10.1073/pnas.1300558110

### SI Materials and Methods

**Strains, Plasmids, and Medium.** The *Escherichia coli* strain BL21 (DE3) [$F^-$ *ompT* $hsdS_B$ ($r_B^-m_B^-$) *gal dcm* (DE3)] or B834(DE3) [$F^-$ *ompT* $hsdS_B$ ($r_B^-m_B^-$) *dcm met* (DE3)] was used for the expression and purification of the recombinant Mpr1 (sig*m*a1278b gene for *p*roline-analog *r*esistance). To overexpress the wild-type (WT) and mutant Mpr1 in *E. coli*, pQE2 vector (Qiagen) harboring the *MPR1* gene in its SacI-HindIII site under the isopropyl-β-D-thiogalactopyranoside (IPTG)-inducible T5 promoter, pQE2-MPR1(SacI-HindIII), was used. The yeast *Saccharomyces cerevisiae* strains with a Σ1278b background used in this study were WT strain L5685 (*MATa ura3-52 trp1 MPR1 MPR2*) (1) and LD1014ura3 (*MATa ura3-52 trp1 mpr1::URA3 mpr2::TRP1 ura3*) (2), which was isolated from the 5-fluoroorotic acid-resistant colonies of strain LD1014 (*MATa ura3-52 trp1 mpr1::URA3 mpr2::TRP1*) (1). The high-copy-number plasmid pYES2 (Invitrogen), which contains the *S. cerevisiae URA3* gene, was used to overexpress Mpr1 under control of the *GAL1* promoter. WT and mutant *MPR1* gene was cloned into the SacI-XhoI site of pYES2.

To express selenomethionine-incorporated Mpr1 in *E. coli*, M9 + selenomethionine (SeMet) medium containing 4% (wt/vol) glucose, 100 mM sodium/potassium phosphate (pH 6.9), 4.3 mM NaCl, 9.3 mM ammonium chloride, 3 mM $MgSO_4$, 0.3 μM $FeCl_3$, 0.5 μM $MnCl_2$, 100 μM $CaCl_2$, 100 μg/mL ampicillin, and 60 μg/mL selenomethionine was used. To express Mpr1 used for the kinetic analysis in *E. coli*, M9+CA medium containing 0.4% (wt/vol) glucose, 65 mM sodium/potassium phosphate, 8.6 mM NaCl, 18.7 mM ammonium chloride, 1 mM $MgSO_4$, 100 μg/mL ampicillin, and 2% (wt/vol) casamino acid was used. To express Mpr1 and its variants in yeast for the determination of L-$\Delta^1$-pyrroline-5-carboxylate (P5C) contents, SCG-U medium containing 2% (wt/vol) galactose as a sole carbon source, 0.67% (wt/vol) yeast nitrogen base without amino acid (Difco), 0.002% (wt/vol) adenine, 0.04% (wt/vol) leucine, 0.0008% (wt/vol) *p*-aminobenzoic acid, 0.008% (wt/vol) of L-arginine, L-aspartic acid, L-glutamine, glycine, inositol, L-methionine, L-phenylalanine, L-serine, L-tryptophan, L-alanine, L-asparagine, L-cysteine hydrochloride, L-glutamic acid, L-histidine, L-isoleucine, L-lysine, L-proline, L-threonine, L-tyrosine, and L-valine were used, and for the evaluation of L-azetidine-2-carboxylic acid (AZC) tolerance, SG medium containing 2% (wt/vol) galactose as a sole carbon source, 0.67% (wt/vol) yeast nitrogen base without amino acid (Difco) with or without 5 mM AZC were used.

Site-directed mutagenesis into *MPR1* was performed using mutagenic primers (Table S5) and pQE2-MPR1(SacI-HindIII) as a template.

**Protein Expression and Purification.** The Mpr1 protein was overexpressed as previously reported (3) with slight modification. Competent cells of *E. coli* strain BL21(DE3) or B834(DE3) were transformed with pQE2-MPR1(SacI-HindIII), expressing Mpr1 with 15 additional N-terminal amino acid residues (MKHHHHHHHMHAGAQ).

***For crystal structure analysis.*** *E. coli* B834(DE3) transformant cells were cultured at 37 °C in M9+SeMet medium. When the absorbance of the culture at 600 nm reached 0.8, Mpr1 was overexpressed by induction with 0.1 mM IPTG at 18 °C for an additional 18 h. The bacterial cell pellet was washed by and suspended in 20 mM sodium phosphate buffer (pH 7.4) containing 500 mM NaCl (buffer A) and then disrupted by sonication using Sonifier 450 (BRANSON). The cell lysate was subjected to centrifugation at 6,000 × *g* for 20 min and filtration to remove cell debris. The resulting cell-free extract was applied to a Ni-affinity column (HisPrep FF 16/10; GE Healthcare Bio-Sciences) equilibrated with buffer A, contaminant proteins were washed away by buffer A containing 80 mM imidazole, and then the bound proteins were eluted using a linear gradient of 80–500 mM imidazole. Fractions containing active Mpr1 were pooled and dialyzed against 20 mM sodium phosphate buffer (pH 7.0) containing 150 mM NaCl, and then His-tag of Mpr1 was digested by the TAGZyme system (Qiagen) at 20 °C for 1 h. After digestion, Mpr1 solution was subjected to Ni-affinity chromatography to remove digested His-tag and undigested His-tagged Mpr1 using a linear gradient of 0–500 mM imidazole. Fractions containing tag-free Mpr1 were pooled and dialyzed against 50 mM Tris·HCl buffer (pH 7.5) containing 1 mM EDTA, 10 mM imidazole, and 10% (wt/vol) glycerol (buffer DEAE A). The solution containing tag-free Mpr1 was applied onto an anion-exchange column (HiPrep DEAE FF 16/10, GE Healthcare Bio-Sciences), and the bound proteins were eluted using a linear gradient of 0–1,000 mM sodium chloride. The eluted enzyme was dialyzed against 10 mM Tris·HCl and concentrated to 4 mg/mL using Amicon Ultra (10-kDa cutoff) and used for the crystallization described below. The removal of the N-terminal His-tag and the introduction of selenomethionine into the purified protein were confirmed by N-terminal amino acid analysis using the ABI 492 cLC Procise Protein Sequencing System (Applied Biosystems) and MALDI-TOF mass spectrometry, respectively. The purity of Mpr1 was determined by SDS/PAGE.

***For enzyme assay.*** Expression and purification of Mpr1 used for enzyme assay was performed by the same procedure as described above with slight modifications. The BE21(DE3) transformant cells were cultured in M9+CA medium. After the first chromatography using Ni-Sepharose 6 Fast Flow (GE Healthcare Bio-Sciences), the purified enzyme was directly used for enzyme assay.

**Crystallization.** Crystals of SeMet-Mpr1 were grown by the sitting-drop vapor-diffusion technique using a Cryschem crystallization plate (Hampton Research) at 293 K. One microliter of Mpr1 solution was mixed with 2 μL of reservoir solution and 1 μL of 50 mM AZC solution. The volume of the reservoir solution in the well was 1,000 μL. The optimal condition, in which the reservoir solution contained 100 mM Bistris-HCl (pH 5.5), 240 mM $MgCl_2$, and 20.5% (wt/vol) PEG 3350, yielded compact and mechanically stable crystals.

**Data Collection, Structure Determination, and Refinement.** ***Leu87SeMet-Mpr1.*** The crystals obtained were transferred stepwise into a cryoprotective solution containing 25% (wt/vol) PEG 400 and flash-cooled at 100 K. Diffraction tests of the crystals were performed using a Rigaku R-AXIS VII detector equipped with a Rigaku FR-E X-ray generator. For the structure determination, X-ray diffraction data were collected using a Rayonix MX225HE CCD detector installed on a BL41XU beamline at SPring-8. All data were processed and scaled using HKL-2000 (4). The crystal belongs to the space group $P3_112$ with a Matthews coefficient ($V_M$) of 2.43 $Å^3$/Da, suggesting a solvent content of 49.3%, assuming that three proteins are present in the asymmetric unit. Phases were calculated by a single-wavelength anomalous dispersion method using data collected at the peak wavelength of selenium. Selenium positions were located using the program SOLVE (5), and phase refinement by solvent flattening was performed with RESOLVE (6). The built model was refined through

alternating cycles using the Coot (7) and Refmac (8) programs. The model was refined to 2.1-Å resolution.

***WT-Mpr1.*** Crystallization and data collection of the wild-type crystal ($P3_112$, AZC-soaked) were carried out as previously described (3). The crystal structure of the wild-type enzyme was solved by molecular replacement using the program PHASER (9). The model of the SeMet mutant was used as a search model. The molecular replacement solution was readily obtained and was rebuilt using ARP/wARP (10). This crystal was a partial merohedral twin with a twin fraction of 0.27. Subsequently, the built model was refined using Coot and Refmac as described above, and the final twin refinement was performed with the program PHENIX (11). In the final model, the main-chain dihedral angles for all residues are in the favored regions (97.9%) or in the allowed regions (2.1%). The final $R_{work}$ and $R_{free}$ were 0.153 and 0.185, respectively. The crystals of Mpr1 in complex with *cis*-4-hydroxy-L-proline (CHOP) were prepared as follows: The Mpr1 crystals were soaked in a cryoprotectant solution containing 10 mM CHOP, 20% (wt/vol) PEG 400, and 15% (wt/vol) glycerol for 1 h at 20 °C before cryocooling. Data for the crystal were collected after flash-cooling using an ADSC Quantum 270 on synchrotron beam line BL-17A at the Photon Factory and KEK-Japan. Analysis of merging statistics and systematic absences using iMosflm (12) showed that the crystals belonged to space group $P2_1$ with the unit-cell parameters $a = 80.3$, $b = 229.3$, $c = 84.8$ Å, and $\beta = 90.9°$. Cumulative intensity distributions indicated no twinning. The crystal structure of the Mpr1-CHOP complex was also solved by molecular replacement, and the refinement was carried out using Coot and PHENIX. In the final model, the main-chain dihedral angles for all residues except Asn178 and Trp182 of chain D are in the favored regions (98.0%) or the allowed regions (1.9%). The loop containing the residues 178–182 showed different conformations in each subunit molecule in the asymmetric unit, probably because of the interaction in the crystal packing. The final $R_{work}$ and $R_{free}$ values of the complex crystal were 0.166 and 0.215, respectively. A summary of data collection and refinement statistics is also given in Table S3. All of the atomic structures of Mpr1 (Leu87SeMet-Mpr1, WT-Mpr1, and WT-Mpr1-CHOP) have been deposited in the Protein Data Bank (codes 3W91, 3W6S, and 3W6X, respectively).

**Acetyltransferase Assay.** The acetyltransferase activity was assayed as described previously (2) using a DU-800 spectrophotometer (Beckman Coulter) with slight modifications. The reaction mixture to determine the specific activity contained 50 mM Tris·HCl (pH 7.5), 5 mM AZC, 100 μM acetyl-CoA (AcCoA), and an appropriate amount of Mpr1. To determine the kinetic parameters for AZC, the concentration of AZC was varied from 1 to 5 mM at the fixed concentration of AcCoA (100 μM). To determine the kinetic parameters for AcCoA, the concentration of AcCoA was varied from 1 to 100 μM at the fixed concentration of AZC (5 mM). To analyze the pH profile, the 50 mM of Tris·HCl (pH 6.94–8.89) or 2-(*N*-morpholino)ethanesulfonic acid (pH 5.81–7.26) was used as a buffer solution. Using the initial velocity at each point, the kinetic parameters were calculated by the curve-fitting method following Eq. **1** for wild type and Eq. **2** for mutant enzymes in GraphPad Prism version 6 for Mac (www.graphpad.com).

$$v = \frac{V\cdot[\mathrm{S}]}{K_\mathrm{m} + [S]\cdot\left(1 + \frac{[\mathrm{S}]}{K_\mathrm{i}}\right)} \quad [1]$$

$$v = \frac{V\cdot[S]}{K_m + [S]} \quad [2]$$

In the equations, $v$ is the initial velocity, $V$ is the maximum velocity, $K_\mathrm{m}$ is Michaelis–Menten constant, and $K_\mathrm{i}$ is the inhibition constant. To evaluate the kinetic mechanism of the Bi-Bi reaction by Mpr1, the concentration of AZC was varied from 0.5 to 3 mM in the presence of the varied concentration of AcCoA from 1 to 100 μM.

**Functional Analysis of the Mpr1 Mutants in Yeast.** *S. cerevisiae* strain LD1014ura3 harboring the empty vector or overexpressing WT, Asn135Asp, or Asn178Asp-Mpr1 was cultured in SCG-U liquid medium containing galactose as the sole carbon source to overexpress Mpr1. After cultivation, the serial dilutions were spotted onto SG agar medium in the presence or absence of 5 mM AZC to examine the growth phenotype. To determine intracellular P5C content, yeast cells were exposed to heat stress (at 39 °C for 5 h) after the cultivation described above. Subsequently, the cells were collected and washed by 0.9% (wt/vol) NaCl and suspended in 1 N HCl solution, and then P5C was extracted at 100 °C for 20 min. Four hundred microliters of the supernatant, 200 μL of 2.4 N perchloric acid, and 200 μL of 2% (wt/vol) ninhydrin aqueous solution were mixed and incubated at 100 °C for 15 min. After centrifugation, the resultant supernatants were removed and the precipitation was dissolved in ethanol. The absorbance of the ethanol solution was measured at 510 nm, and the concentration of the P5C-ninhydrin complex was calculated using the molar absorbance coefficient (16,500 $M^{-1}\cdot cm^{-1}$) (13).

**Sedimentation-Velocity Ultracentrifugation Experiments.** Sedimentation was performed at 20 °C using a Beckman Coulter Optima XLA analytical ultracentrifuge equipped with an An-60 Ti rotor and double-sector centerpieces. Purified samples were dissolved in 100 mM Tris·HCl (pH 7.5) with/without 50 mM AZC at a sample concentration of 100 μM and then centrifuged at 30,000 × *g*. Radial absorbance scans were measured every 10 min, and the resultant data were analyzed using the SEDFIT program.


1. Shichiri M, Hoshikawa C, Nakamori S, Takagi H (2001) A novel acetyltransferase found in *Saccharomyces cerevisiae* Σ1278b that detoxifies a proline analogue, azetidine-2-carboxylic acid. *J Biol Chem* 276(45):41998–42002.
2. Nomura M, Takagi H (2004) Role of the yeast acetyltransferase Mpr1 in oxidative stress: Regulation of oxygen reactive species caused by a toxic proline catabolism intermediate. *Proc Natl Acad Sci USA* 101(34):12616–12621.
3. Hibi T, Yamamoto H, Nakamura G, Takagi H (2009) Crystallization and preliminary crystallographic analysis of *N*-acetyltransferase Mpr1 from *Saccharomyces cerevisiae*. *Acta Crystallogr Sect F Struct Biol Cryst Commun* 65(Pt 2):169–172.
4. Otwinowski Z, Minor W (1997) Processing of X-ray diffraction data collected in oscillation mode. *Methods Enzymol* 276:307–326.
5. Terwilliger TC, Berendzen J (1999) Automated MAD and MIR structure solution. *Acta Crystallogr D Biol Crystallogr* 55(Pt 4):849–861.
6. Terwilliger TC (2000) Maximum-likelihood density modification. *Acta Crystallogr D Biol Crystallogr* 56(Pt 8):965–972.
7. Emsley P, Cowtan K (2004) Coot: Model-building tools for molecular graphics. *Acta Crystallogr Sect D Biol Crystallogr* 60(Pt 12 Pt 1): 2126–2132.
8. Murshudov GN, Vagin AA, Dodson EJ (1997) Refinement of macromolecular structures by the maximum-likelihood method. *Acta Crystallogr D Biol Crystallogr* 53(Pt 3):240–255.
9. McCoy AJ, et al. (2007) Phaser crystallographic software. *J Appl Cryst* 40(Pt 4):658–674.
10. Perrakis A, Harkiolaki M, Wilson KS, Lamzin VS (2001) ARP/wARP and molecular replacement. *Acta Crystallogr D Biol Crystallogr* 57(Pt 10):1445–1450.
11. Adams PD, et al. (2010) PHENIX: A comprehensive Python-based system for macromolecular structure solution. *Acta Crystallogr D Biol Crystallogr* 66(Pt 2):213–221.
12. Battye TG, Kontogiannis L, Johnson O, Powell HR, Leslie AG (2011) iMOSFLM: A new graphical interface for diffraction-image processing with MOSFLM. *Acta Crystallogr D Biol Crystallogr* 67(Pt 4):271–281.
13. Ravikumar H, Devaraju KS, Shetty KT (2008) Effect of pH on spectral characteristics of P5C-ninhydrin derivative: Application in the assay of ornithine amino transferase activity from tissue lysate. *Indian J Clin Biochem* 23(2):117–122.

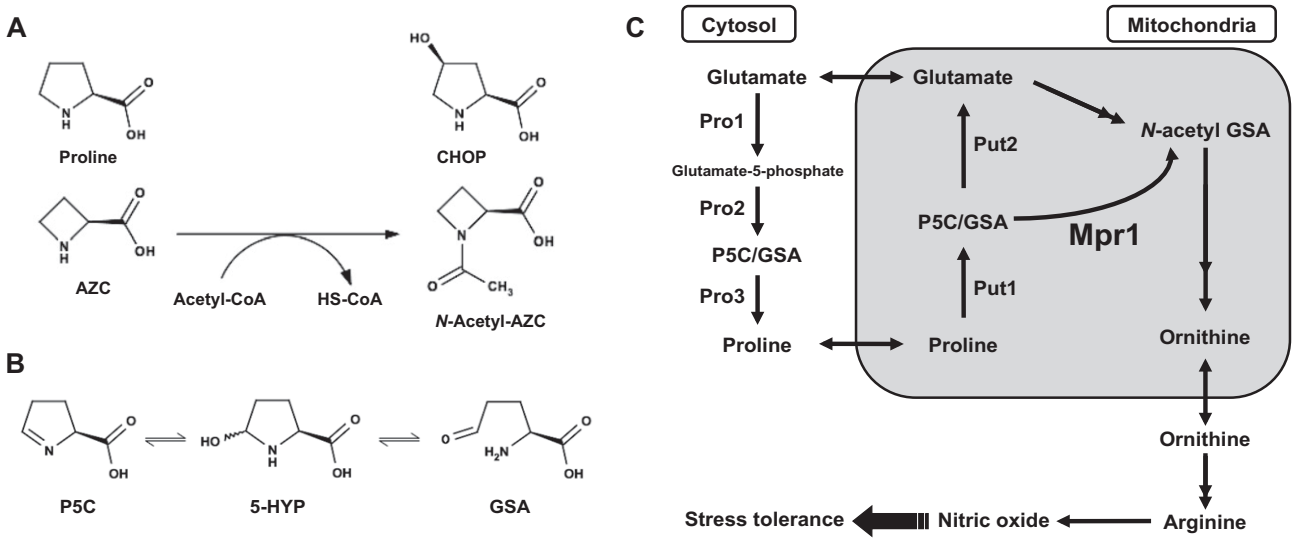


**Fig. S1.** Metabolism of AZC, CHOP, and L-proline. (*A*) Proposed scheme for the AZC acetyltransferase reaction by Mpr1. CHOP is also acetylated in the same manner. (*B*) The equilibrium reaction between P5C and L-glutamate-γ-semialdehyde (GSA). P5C and GSA are converted into each other depending on environmental pH by the addition of one water molecule through the unstable intermediate 5-hydroxy-L-proline (5-HYP). (*C*) Metabolic pathways of L-proline and L-arginine in *S. cerevisiae*. Protein names: Pro1, γ-glutamyl kinase; Pro2, γ-glutamyl phosphate reductase; Pro3, P5C reductase; Put1, proline oxidase; Put2, P5C dehydrogenase; Mpr1, P5C/GSA *N*-acetyltransferase.

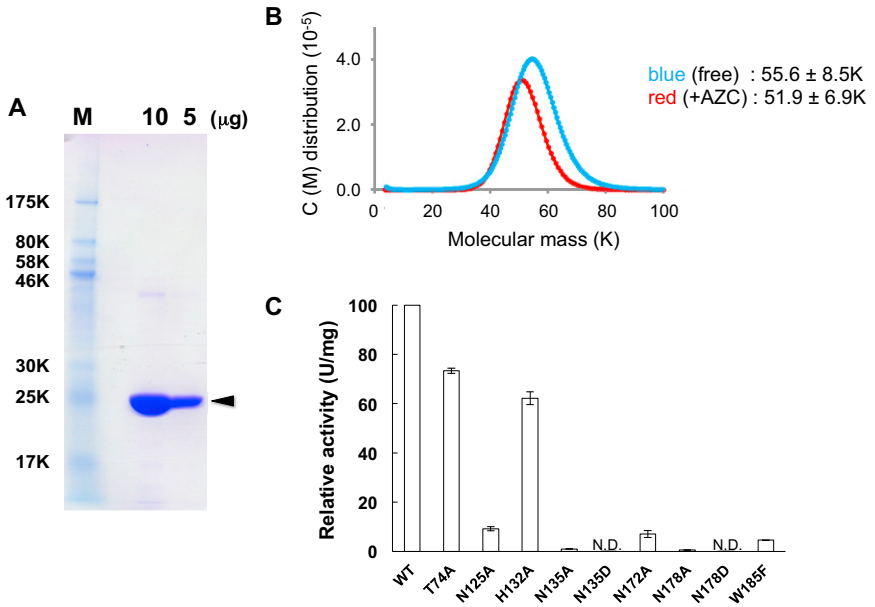


**Fig. S2.** Purity, oligomeric state, and enzymatic analyses of Mpr1. (*A*) The purity of the Leu87SeMet mutant Mpr1, in which His-tag has been already removed, was examined with SDS/PAGE and Coomassie Brilliant Blue staining. The indicated amount of protein was loaded on SDS/PAGE. The black arrowhead indicates the position of the Leu87SeMet mutant Mpr1. Molecular mass standards (M) are shown at the left. (*B*) Ultracentrifugation of Mpr1. Mpr1 exhibited the molecular mass corresponding to a dimer structure either in the presence or the absence of AZC. (*C*) The specific activity of each variant Mpr1 was determined at the fixed concentrations of AZC (5 mM) and AcCoA (100 μM) and was expressed as a percentage of WT-Mpr1. The values are the means and SDs from three independent experiments. N.D. (not detected) indicates that the specific activity was less than 0.003 U/mg (less than 0.0035% of WT-Mpr1).

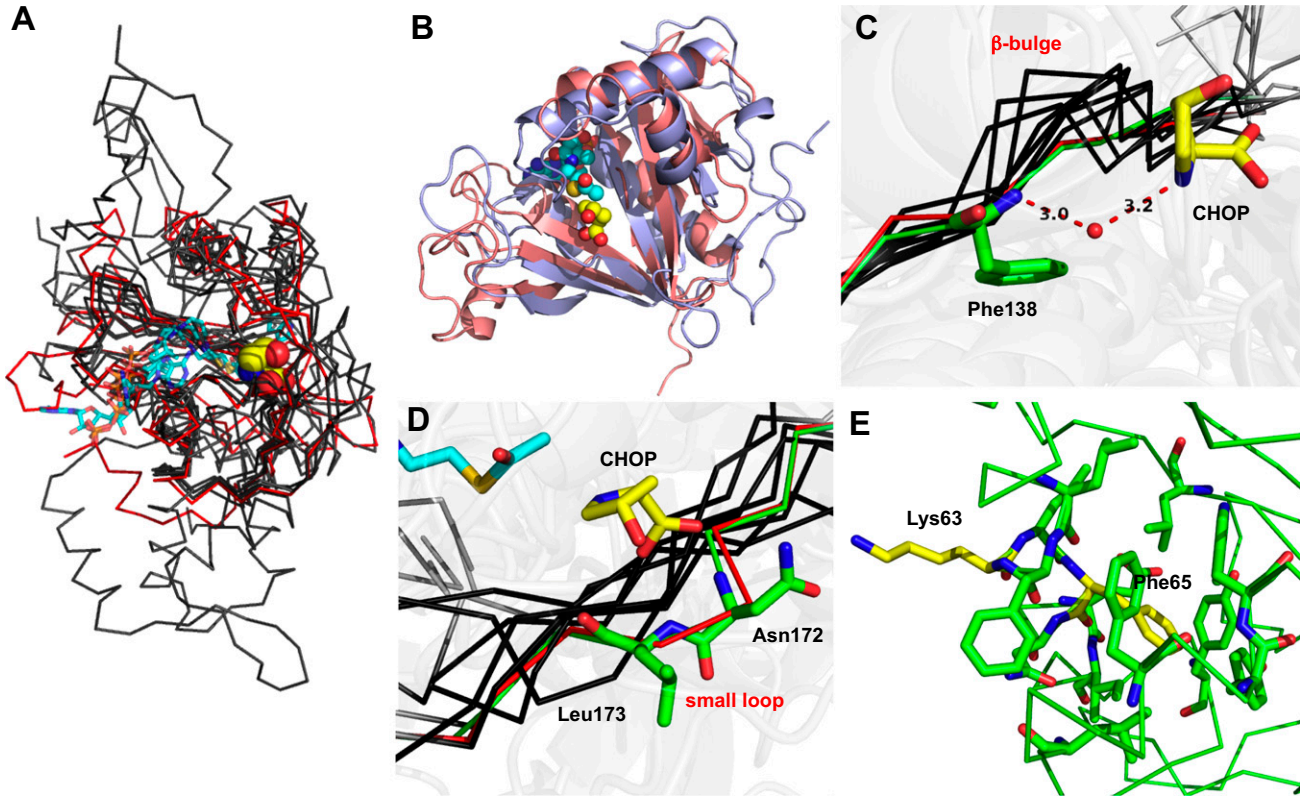


**Fig. S3.** The overall and local structure of Mpr1. (*A*) The superimposition of Mpr1 with other typical Gcn5-related *N*-acetyltransferase (GNAT) proteins (PDB ID codes 2CNS, 1M4I, 1CJW, 1I1D, 1FY7, and 1OZP). Proteins are shown by the ribbon model. Ligands (CoA derivatives) bound to other GNAT proteins and CHOP bound to Mpr1 are shown by stick and sphere models, respectively. Each structure overlaps nicely in the region around CoA ligands. (*B*) The structure of WT-Mpr1-CHOP (light blue) is superimposed with that of an aminoglycoside 6′-*N*-acetyltransferase from *Enterococcus faecium* (PDB ID 1B87) (salmon pink). AcCoA in the structure 1B87 and CHOP in the structure of WT-Mpr1-CHOP are shown as a sphere model. (*C* and *D*) Mpr1, the structure 4H89, and other proteins (PDB ID codes 1B87, 2CNS, 1M4I, 1CJW, 1I1D, 1FY7, and 1OZP) are shown by green, red, and gray, respectively, in the focused region on each panel. (*C*) The β-bulge structure of Mpr1 and other GNAT proteins. Phe138 and CHOP bound to Mpr1 are shown as a stick model. A red ball indicates a water molecule bound to CHOP and Mpr1. The β-bulge structures are observed in all proteins except for Mpr1 and 4H89. (*D*) The small loop structure for substrate recognition in Mpr1. AcCoA in the structure 1B87 and CHOP bound to Mpr1, Asn172, and Leu173 are also shown by stick model. Only Mpr1 and 4H89 exhibit the small loop structure to recognize CHOP. (*E*) Lys and Phe at positions 63 and 65, respectively, are shown by the yellow stick model. The side chain of Phe65 is surrounded by hydrophobic residues, whereas Lys63 has no interaction partners.

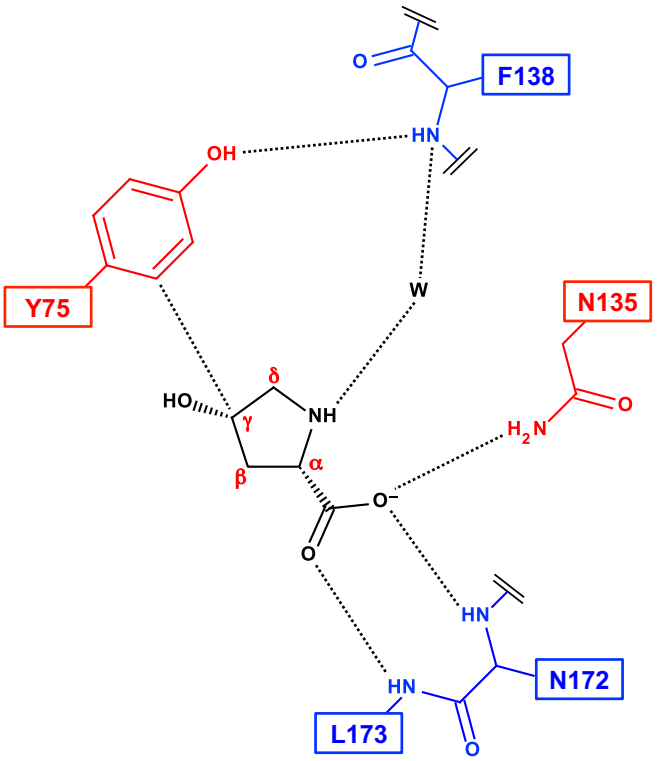


**Fig. S4.** Scheme of CHOP binding to Mpr1. CHOP-binding site on Mpr1 is schematically illustrated. CHOP is shown by black color, and red letters indicate the carbon atom numbering of CHOP. The red and blue residues interact with the substrates through their side chain and backbone, respectively. Black dotted lines show the possible van der Waals interaction and hydrogen bonds. CHOP binds to the side chain of Asn135 and the backbone amide N-H group of Asn172 and Leu173 through its carboxyl group and to a water molecule bound to Phe138 through its amine group. CHOP also forms a van der Waals contact with the phenolic side chain of Tyr75 through its Cγ atom.

**Table S1. Mass spectrometry analysis**

| Mpr1 | Detected mass (*m/z*) | Calculated mass (*m/z*) |
|---|---|---|
| WT | 26,484.808 | 26,488.77 |
| Leu87SeMet | 26,642.980 | 26,647.51 |

The difference of the detected mass of Leu87SeMet-Mpr1 from that of WT-Mpr1 is about 158, which is consistent with the calculated difference, indicating that the incorporation rate of selenomethionine into the Leu87-SeMet mutant Mpr1 is almost 100%.

**Table S2. N-Terminal sequencing analysis**

| Position | Detected amino acid |
|---|---|
| First | Gly |
| Second | Ala |
| Third | Gln |

The results of N-terminal sequencing analysis of the Leu87SeMet mutant Mpr1 after the reaction to cleave the fused His-tag showed Gly-Ala-Gln sequence from N terminus, indicating that the fused His-tag was removed and the resultant protein has a homogenous N terminus derived from the cloning artifact.

**Table S3. X-ray data collection and refinement statistics**

| Data | Leu87SeMet-Mpr1 | WT-Mpr1 | WT-Mpr1-CHOP |
|---|---|---|---|
| Data collection | | | |
| Wavelength (Å) | 0.9792 | 0.9793 | 0.9851 |
| Space group | $P3_112$ | $P3_112$ | $P2_1$ |
| *a*, *b*, *c* (Å), β (°) | 83.6, 83.6, 192.4, 120 | 83.9, 83.9, 193.8, 120 | 80.3, 229.3, 84.8, 90.9 |
| Resolution (Å)* | 50–2.10 (2.18–2.10) | 48.3–1.90 (2.00–1.90) | 56.9–2.30 (2.40–2.30) |
| Measured reflections | 501,253 | 490,882 | 507,672 |
| Unique reflections | 45,346 | 61,875 | 134,196 |
| Redundancy | 11.1 (10.0) | 7.9 (7.7) | 3.8 (3.5) |
| Completeness (%) | 99.1 (96.3) | 100.0 (100.0) | 99.0 (99.0) |
| $I/(\sigma I)$ | 42.5 (9.9) | 26.0 (7.1) | 8.0 (2.5) |
| $R_{merge}$ (%) | 5.9 (21.4) | 6.0 (28.7) | 9.8 (45.3) |
| Refinement | | | |
| Resolution (Å) | 50.0–2.1 | 48.3–1.9 | 50.0–2.3 |
| $R_{work}/R_{free}$† | 0.198/0.250 | 0.166/0.187 | 0.166/0.215 |
| Atoms | | | |
| Protein | 5,500 | 5,300 | 21,779 |
| Ligand | — | 43 | 203 |
| Water | 198 | 228 | 602 |
| B-factor (Å$^2$) | | | |
| Protein | 12.6 | 30.4 | 38.1 |
| Ligand | — | 34.6 | 56.2 |
| Water | 12.0 | 35.8 | 34.6 |
| rmsd | | | |
| Bond lengths (Å) | 0.015 | 0.008 | 0.014 |
| Bond angles (°) | 1.39 | 1.02 | 1.36 |
| Twin law | | *h*, *k*, *l* and -*h*, -*k*, *l* | |
| Twin fraction | | 0.27 | |

*Values in parentheses are the statistics for the highest resolution shell of data.
†$R_{free}$ was calculated with the 5% of reflections set aside randomly throughout the refinement.

**Table S4. 3D homology search using Dali server**

| Rank | PDB ID | rmsd | Host |
|---|---|---|---|
| 1 | 3DR6 | 2.1 | *Salmonella enterica* subsp. *enterica serovar Typhimurium* str. LT2 |
| 2 | 3DR8 | 2.1 | *S. enterica* subsp. *enterica serovar Typhimurium* str. LT2 |
| 3 | 1VHS | 2.4 | *Bacillus subtilis* |
| 5 | 1YVO | 2 | *Pseudomonas aeruginosa* PAO1 |
| 6 | 2JLM | 2.3 | *Acinetobacter baylyi* |
| 8 | 2J8M | 2 | *P. aeruginosa* |
| 9 | 2J8R | 2.2 | *P. aeruginosa* |
| 14 | 2J8N | 2.2 | *P. aeruginosa* |
| 16 | 1YR0 | 2.1 | *Agrobacterium tumefaciens* |
| 20 | 3LD2 | 2.2 | *Streptococcus mutans* UA159 |
| 23 | 2BL1 | 2 | *P. aeruginosa* |
| 28 | 2GE3 | 2.4 | *A. tumefaciens* |
| 34 | 1GHE | 2.7 | *Pseudomonas syringae pv. tabaci* |
| 37 | 1J4J | 2.7 | *P. syringae* pv. *tabaci* |
| 38 | 2I79 | 2.8 | *Streptococcus pneumoniae* TIGR4 |
| 45 | 2CNM | 2.6 | *S. enterica* subsp. *enterica serovar Typhimurium* str. LT2 |
| 50 | 2AE6 | 2.4 | *Enterococcus faecalis* V583 |
| 59 | 2CNT | 2.7 | *S. enterica subsp. enterica serovar* Typhimurium str. *LT2* |
| 61 | 1N71 | 2.2 | *E. faecium* |
| 65 | 2A4N | 2.3 | *E. faecium* |
| 71 | 1B87 | 2.3 | *E. faecium* |
| 147 | 4FD7 | 3.2 | ***Aedes aegypti*** |
| 153 | 3TFY | 3.2 | ***Homo sapiens*** |
| 168 | 2OB0 | 3.2 | ***H. sapiens*** |

Some results of the 3D homology search using Dali server are listed, and all of them are *N*-acetyltransferases. All proteins listed in roman type are from bacteria, and those in boldface are from eukaryotes. Among the proteins obtained as structurally similar proteins to Mpr1, all that placed high were bacterial *N*-acetyltransferases with the rmsd value of 1.8–2.8 Å. On the other hand, the protein that placed highest derived from a eukaryote ranked 147th and with an rmsd of 3.2 Å, suggesting that the structure of Mpr1 is more similar to those of bacterial *N*-acetyltransferases than to those of eukaryotic *N*-acetyltransferases. This search was performed before the publication of the crystal structure of PDB ID code 4H89.

**Table S5. Mutagenic primers used in this study**

| Mutation | Primer sequence |
|---|---|
| Thr74Ala | 5′-aagtggcaagGCCtatccacaat-3′ |
| | 5′-attgtggataGGCcttgccactt-3′ |
| Asn125Ala | 5′-catcaagcccGCCtatgctccgc-3′ |
| | 5′-gcggagcataGGCgggcttgatg-3′ |
| His132Ala | 5′-gctccgcgttgctcgGCTaattgcaatgctggc-3′ |
| | 5′-gccagcattgcaattAGCcgagcaacgcggagc-3′ |
| Asn135Ala | 5′-gcataattgcGCCgctggctttc-3′ |
| | 5′-gaaagccagcGGCgcaattatgc-3′ |
| Asn135Asp | 5′-gcataattgcGATgctggctttc-3′ |
| | 5′-gaaagccagcATCgcaattatgc-3′ |
| Asn172Ala | 5′-ctctatctttGCCcttgtctttg-3′ |
| | 5′-caaagacaagGGCaaagatagag-3′ |
| Asn178Ala | 5′-gttaccGCTcaagctagttgg-3′ |
| | 5′-ccaactagcttgAGCggtaac-3′ |
| Asn178Asp | 5′-gttaccGATcaagctagttgg-3′ |
| | 5′-ccaactagcttgATCggtaac-3′ |
| Trp185Phe | 5′-ttggaaaataTTTgacaaattaa-3′ |
| | 5′-ttaatttgtcAAAtattttccaa-3′ |
| Leu87Met | 5′-aaacagggattcATGaattattggttt-3′ |
| | 5′-aaaccaataattCATgaatccctgttt-3′ |

The nucleotide sequences of the primers used in this study are shown. The capital letters indicate the mismatched sequences to introduce mutations.